

**PRECIPITATION AND FRESH WATER LENS FORMATION  
IN THE TROPICAL WESTERN PACIFIC**

Jon Schrage  
Creighton University, Omaha, Nebraska

and

C.A. Clayson  
Florida State University, Tallahassee, Florida

**1. INTRODUCTION**

The western equatorial Pacific contains the world's highest open ocean sea surface temperatures (SST). Associated with these high SSTs is deep atmospheric convection, culminating in a maximum in global oceanic rainfall. The SST is in turn dependent on many properties of the air/sea interface, such as the surface fluxes of heat, moisture and momentum. The ocean mixed layer structure also plays a significant role in determination of the SST. As a result of the large amount of precipitation in the tropical western Pacific warm pool, substantial salinity stratification exists within the upper ocean.

The effects of rainfall on the upper ocean on the vertical scale include an enhancement of free convection due to the typically cooler temperature of the rainfall and a decrease in forced convection due to the increased stable stratification of the upper layer (e.g. Price 1979). This increased stability can lead to a shallower mixed layer (Lukas and Lindstrom, 1990), and the resulting SSTs are then more sensitive to surface heat flux variability. In addition to the local effects, horizontal variability in rainfall can lead to horizontal salinity and density gradients, which may then initiate dynamic ocean adjustment.

Convection and the resultant precipitation in the tropical Pacific extends over a wide range of temporal and spatial scales. Precipitation can occur over as small an area as one cumulus cloud and last less than an hour, or can be associated with squalls, mesoscale convective systems, two-day oscillations, or larger convective variability. Resultant salinity variations should also then be associated with the varying temporal and spatial scales of precipitation. Regions of lowered salinity water associated with individual cloud-scale and squall-scale convective variability have been observed and studied by several researchers during the Tropical Ocean Global Atmosphere – Coupled Ocean Atmosphere Response Experiment (TOGA COARE) (Webster and Lukas, 1992). Analysis of upper ocean profile data obtained during the Intensive Observation Period (IOP) of TOGA COARE has highlighted the formation of these patches of fresher and colder surface water produced

by localized rainfall (Paulson and Lagerloef, 1993; Soloviev et al. 1993; Tomczak 1995; Wijesekera et al. 1999). These areas of fresh surface water, termed “freshwater lenses”, are characterized by depressions in SST of 0.5 - 1.5 °C and in sea surface salinity (SSS) of 0.2 - 2 psu (Lukas, 1990; Asghar and Lukas, 1995). The freshwater can extend to depths well within the mixed layer; Tomczak (1995) found penetration depths of 20 m. Brainerd and Gregg (1997) using microstructure data in the western tropical Pacific observed local freshwater lens formation due to precipitation, and that these lenses lasted on the order of a few days. Wijesekera et al. (1999) also observed the formation of a freshwater lens on the order of roughly 20 km that was coincident with a strong rainfall event, and found evidence of the low-salinity anomaly down to 40 m. The lifetime and depth of these lenses depended on the convective regime in which the precipitation was occurring; lenses occurring during the strong winds of the westerly wind burst were deeper but shorter-lived. These fairly localized freshwater lenses also appear to have been affected by advection in several cases (Smyth et al., 1996; Tomczak 1995). The suppression of surface-generated turbulence near the bottom of a freshwater lens was measured by Smyth et al. (1996).

Salinity variability on a larger scale (seasonal to interannual) has also been studied. Ando and McPhaden (1997) evaluated in situ temperature and salinity data in the tropical Pacific over the years 1976 to 1994 and concluded that on interannual time scales feedbacks between upper ocean salinity, temperature, and precipitation were possible. A similar interannual dependence of surface layer salinity and temperature stratification was seen in the model results of Vialard and Delecluse (1998a, b). However, salinity variability associated with convective (and precipitation) variability from the mesoscale to the seasonal scale is less well understood, although changes on the order of days to weeks has been observed (Lukas, 1990). Resulting ocean dynamic adjustment, as well as concurrent upper ocean stability structure and sea surface temperature variability is also not well understood.

In this talk we will describe salinity variability associated with scales from 30 km to several degrees as shown in results from a three-dimensional ocean model in the western Pacific. The spatial and temporal extent of the lenses, their mechanisms of formation and destruction, and the resultant effects on ocean dynamics and sea surface temperature will also be evaluated.

---

\*Corresponding author address: Jon Schrage, Department of Environmental and Atmospheric Science, Creighton University, 2500 California Plaza, Omaha, NE 68178; email: [jon@creighton.edu](mailto:jon@creighton.edu)

Within this abstract we describe the three-dimensional ocean model used for this research, as well as initialization and forcing fields, and show results for one moderate-sized lens.

## 2. MODEL AND DATA DESCRIPTION

The three-dimensional equatorial Pacific ocean model used in this study is a high-resolution primitive equation model that has a comprehensive ocean mixed layer submodel plus detailed parameterization of the processes that occur at the air/sea interface. It is based on the University of Colorado version (CUPOM) of the Princeton sigma-coordinate, free surface, 3D ocean model (Blumberg and Mellor, 1987) described by Kantha and Piacsek (1993). The model incorporates an accurate ocean mixed layer model described by Kantha and Clayson (1994) that uses second moment turbulence closure, and includes improved parameterizations that have been developed based upon large eddy simulations. The mixed layer model has been validated over many time scales and in many locations, including data from the TOGA COARE Pilot Cruise (Kantha and Clayson 1994) and the IOP (Webster et al. 1996). The full three-dimensional version of the model has also been applied to a number of locations in the global oceans (e.g., Clifford et al. 1997, Horton et al. 1997). The tropical Pacific version of the model has a fine horizontal resolution ( $1/3^\circ$  in the zonal direction) in the western Pacific warm pool region, changing to a fairly coarse resolution ( $1^\circ$  in the zonal direction) in the eastern and central Pacific. The resolution in the meridional direction is  $1/3^\circ$  in regions close to the equator telescoping to  $1^\circ$  at the edge of the model domain ( $20^\circ\text{N}$ ,  $20^\circ\text{S}$ ). This version of the model is run at a fine vertical resolution (38 levels with 10 m resolution in the upper 250 m, less than 1 m near the surface) to resolve the mixed layer and the equatorial undercurrent. Radiational boundary conditions are employed along the northern and southern boundaries of the model to prevent Kelvin waves propagating along the lateral boundaries from being deflected into the model domain.

The model simulations performed here were for the period of 1 January 1998 through 1 January 1999. The ocean model has been initialized using monthly average temperature, salinity, and velocity fields derived from weekly analysis using the NCEP Ocean-Data Assimilation System (ODAS). The data are freely available from NCAR (DSS 277.1) at  $1^\circ$  latitude by  $1.5^\circ$  longitude resolution since 1980. This archive has been described by Ji et al. (1995 a,b) and Derber and Rosati (1989). The sensible and latent heat flux and the momentum flux used for forcing the model were obtained from the European Centre for Medium-Range Weather Forecasts (ECMWF) reanalysis dataset. These analyses are available four times per day at a spatial resolution of  $2.5^\circ$ . The surface

radiative fluxes were obtained from ISCCP analysis (Rossow and Schiffer, 1999), and are available every three hours at a spatial resolution of  $1.0^\circ$ . Precipitation fluxes were obtained from TRMM 3B42 data, and are available daily at a spatial resolution of  $1.0^\circ$ . The model itself is run with a 15 minute timestep.

This ocean model has been developed primarily to reproduce adequately the small-scale variability associated with diurnal and mesoscale atmospheric forcing. Comparisons of the model simulations with the IMET buoy and the TOGA TAO buoy shows that the modeled sea surface temperatures are reasonable and both shorter and longer timescale variability is well represented (Clayson et al. 1998).

## 3. FRESHWATER LENS EXAMPLE

An example of a freshening event in the western equatorial Pacific is shown in Figure 1. These results are for the time period of 17 – 22 January, and the daily-averaged precipitation for this time period is shown in Figure 2. The maximum of precipitation on 17 January was over  $55 \text{ mm day}^{-1}$ , and was roughly centered at  $152.5^\circ\text{E}$  and  $1.5^\circ\text{S}$ . The results of this rainfall can be seen in the growing spatial coverage of freshwater with salinities less than  $34.95 \text{ psu}$  between 17 January and 18 January. This fresher area was then reduced in size and was nearly non-existent by 22 January, even though a few periods of continued precipitation occurred. Smaller patches of even fresher water (with salinities less than  $34.9 \text{ psu}$ ) can be seen within this larger freshening, on scales of less than  $1^\circ$ . However, the location of the maximum in rainfall and the minimum in salinity do not coincide, possibly due to advection, which during this time period is westward, with a small southward component (surface currents are shown in Figure 3). The advection is consistent with the location of the salinity minima compared to the precipitation maximum.

The abrupt change in sea surface salinity can be seen by evaluating the change in salinity over the upper 30 m at the point  $152^\circ\text{E}$ ,  $2.7^\circ\text{S}$  (Figure 4). This is the location of the larger of the small-scale fresh lenses, and is well to the southwest of the precipitation maximum. During the strong precipitation on 17 January, as mentioned, the currents in this region were southwestward, consistent with the advection of the lens into this region. The extent to which advection may have played a role can be seen by comparison of the time series of salinity with depth and precipitation; the freshening of the surface layer on 17 January is roughly coincident with the onset of precipitation. However, there are several other precipitation events that occur after 17 January (on 20 January and to a lesser extent from 23 to 25 January), and neither of these result in a fresh lens formation. The currents had weakened by 19 January, and were roughly southeastward, so no water from the smaller rain event maximum on January 20 was entering this region. Formation of the strong lens (the effects of which can be seen down to roughly 30 m) on 17 – 18

January is also coincident with a minimum of surface wind stress (see Figure 4). This is also a possible cause of the stronger lens on this day than the following time periods, which have stronger winds.

The smaller lenses have a lifetime of less than two days. Possible mechanisms for this are the advection of higher saline water from the southwest, and the local effect of mixing. These mechanisms will be further discussed in the presentation. As expected, the larger pool of fresh water has a longer lifetime, with minimum sea surface salinity features evident for longer than one week.

Changes in the upper ocean temperature at 152 °E, 2.7 °S are also shown in Figure 4. Maximums in surface heat flux are found between 15 and 18 January and 21 through 25 January. However, the only days with strong warming during daytime conditions are 15 January and 17 January, both of which are coincident with strong upper ocean salinity stratification.

#### 4. SUMMARY

Several scales of salinity variability are evident in the case discussed within this abstract. Within the larger-scale upper ocean freshening several lenses of less than 1° in diameter are seen. These lenses are however not coincident with the maximum in precipitation, but are possibly a result of the advection of the water from the precipitation maximum region. A further analysis of this case and other cases will be shown in the presentation.

**Acknowledgments.** This work was supported by the NASA TRMM program under grant NAG5-9822.

#### 5. REFERENCES

Ando, K. and M. J. McPhaden, 1997: Variability of surface layer hydrography in the tropical Pacific Ocean. *J. Geophys. Res.*, **102**, 23063-23078.

Blumberg, A.F. and G.L. Mellor, 1987: A description of a three-dimensional coastal ocean circulation model, in *Three-Dimensional Coastal Ocean Models*, 4, pp 208, American Geophysical Union, Washington, D.C.

Clayson, C.A., J. A. Curry, and C. W. Fairall, 1996: Evaluation of turbulent fluxes at the ocean surface using surface renewal theory. *J. Geophys. Res.*, **101**, 28,503-28,53.

Clayson, C. A., L. H. Kantha and P. J. Webster, 1998: Spatial and temporal variability in a numerical ocean model of the tropical Pacific. AGU 1998 Ocean Sciences Meeting, San Diego, CA, February 9-13.

Clifford, M., C. Horton, J. Schmitz, and L. Kantha, 1997: An oceanographic nowcast/forecast system for the Red Sea, *J. Geophys. Res.*, **102**, 25,101-25,122.

Derber, J. D. and A. Rosati, 1989: A global oceanic data assimilation system. *J. Phys. Oceanogr.*, **19**, 1333-1347.

Horton, C., M. Clifford, J. Schmitz, and L. Kantha, 1997: A real-time oceanographic nowcast/forecast system for the Mediterranean Sea, *J. Geophys. Res.*, **102**, 25,123-25,156 (Corrections: *J. Geophys. Res.*, **102**, 27,911, 1997, and *J. Geophys. Res.*, **103**, 18,811, 1998).

Ji, M., and T. M. Smith, 1995: Ocean model response to temperature data assimilation and varying surface wind stress: Intercomparisons and implications for climate forecast. *Mon. Wea. Rev.*, **123**, 1811 – 1821.

Ji, M., A. Leetmaa and J. Derber, 1995: An ocean analysis system for seasonal to interannual climate studies. *Mon. Wea. Rev.*, **123**, 460-481.

Kantha, L.H. and C.A. Clayson, 1994: An improved mixed layer model for geophysical applications. *J. Geophys. Res.*, **99**, 25235-25266.

Kantha, L. and S. Piacsek, 1993: Ocean Models in *Computational Science Education Project*. Dept. of Energy, 273-361.

Lukas, R., 1990: The role of salinity in the dynamics and thermodynamics of the western Pacific warm pool, in *Proceedings of US-PRC International TOGA Symposium*, pp. 305-327, China Ocean Press, Beijing.

Lukas, R. and E. J. Lindstrom, 1991: The mixed layer of the western equatorial Pacific Ocean. *J. Geophys. Res.*, **96**, 3343-3357.

Paulson, C. A., and G. Lagerloef, 1993: Fresh surface lenses caused by heavy rain over the western equatorial Pacific Warm Pool during TOGA COARE (abstract). *Eos Trans. Amer. Geophys. Union*, **73**(43), Fall Meet. Suppl., p. 125.

Price, J. F., 1979: Observations of a rain-formed mixed layer. *J. Phys. Oceanogr.*, **9**, 643-649.

Rosow, W.B., and R. A. Schiffer, 1999: Advances in understanding clouds from ISCCP. *Bull. Amer. Meteor. Soc.*, **80**, 2261.

Smyth, W. D., D. Hebert, and J. N. Moum, 1996: Local ocean response to a multiphase westerly wind burst 2. Thermal and freshwater responses. *J. Geophys. Res.*, **101**, 22513-22533.

Soloviev, A., R. Lukas, S. Asghar, and D. Khlebnikov, 1993: Coherent structures near the air-sea interface in the western Pacific Warm Pool (abstract). *Eos Trans. Amer. Geophys. Union*, **73**(43), Fall Meet. Suppl., p. 148.

Tomczak, M., 1995: Salinity variability in the surface layer of the tropical western Pacific Ocean. *J. Geophys. Res.*, **100**, 20499-20515.

Vialard, J. and P. Delecluse, 1998a: An OGCM study for the TOGA decade. Part I: Role of salinity in the physics of the western Pacific fresh pool. *J. Phys. Oceanogr.*, **28**, 1071-1088.

Vialard, J. and P. Delecluse, 1998b: An OGCM study for the TOGA decade. Part II: Barrier-layer formation and variability. *J. Phys. Oceanogr.*, **28**, 1089-1106.

Webster, P. J. and R. Lukas, 1992: TOGA COARE: The Coupled Ocean-Atmosphere Response Experiment. *Bull. Amer. Meteorol. Soc.*, **73**, 1377-1416.

Webster, P.J., C.A. Clayson, and J.A. Curry, 1996: Clouds, radiation, and the diurnal cycle of sea surface temperature in the tropical western Pacific. *J. Clim.*, **9**, 1712-1730.

Wijsekera, H. W., C. A. Paulson, and A. Huyer, 1999: The effect of rainfall on the surface layer during a westerly wind burst in the western equatorial Pacific. *J. Phys. Oceanogr.*, **29**, 612-632.

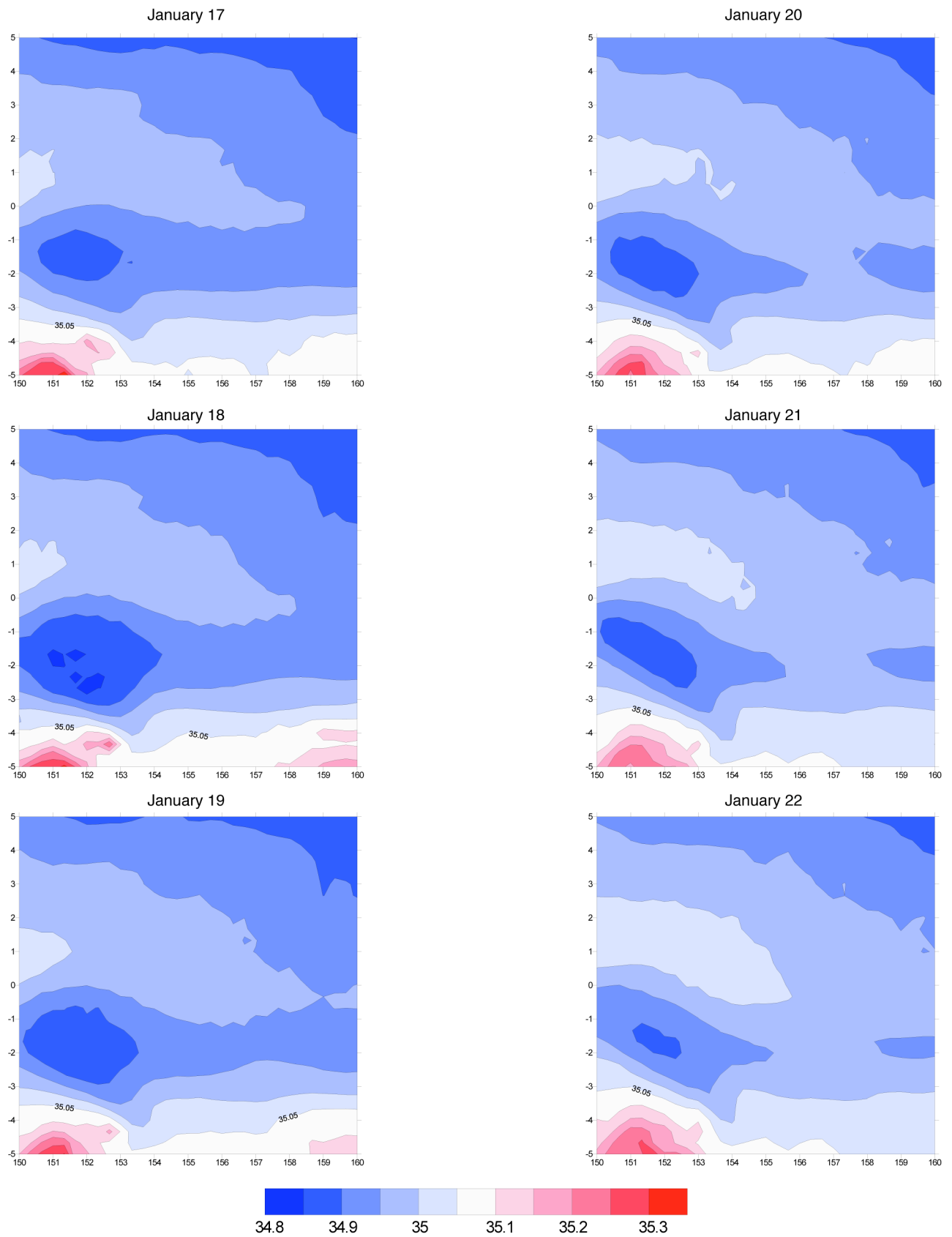


Figure 1. Sea surface salinity variability (in psu) from 17 – 22 January.

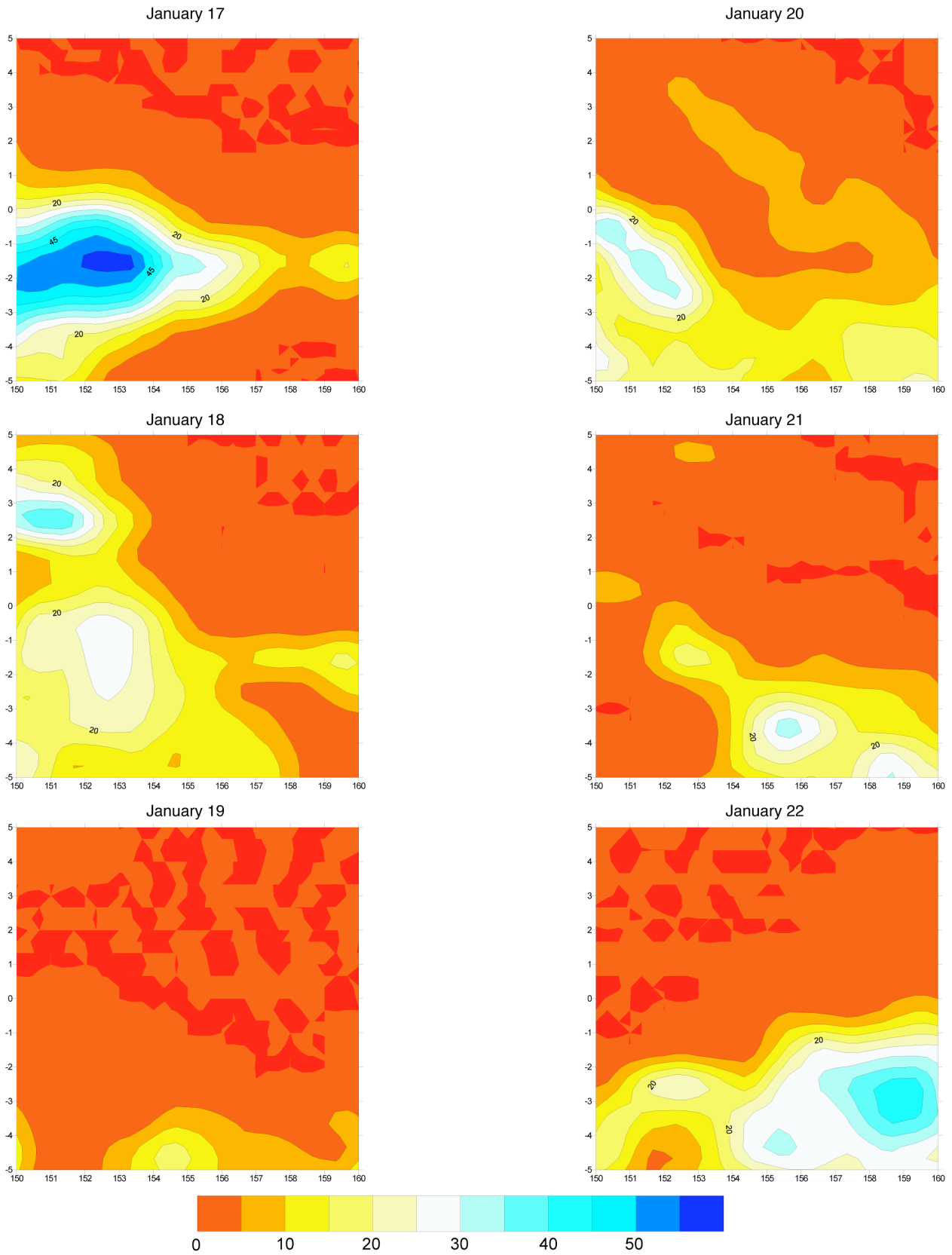


Figure 2. Daily-averaged rainfall (in mm day<sup>-1</sup>) from 17 – 22 January.

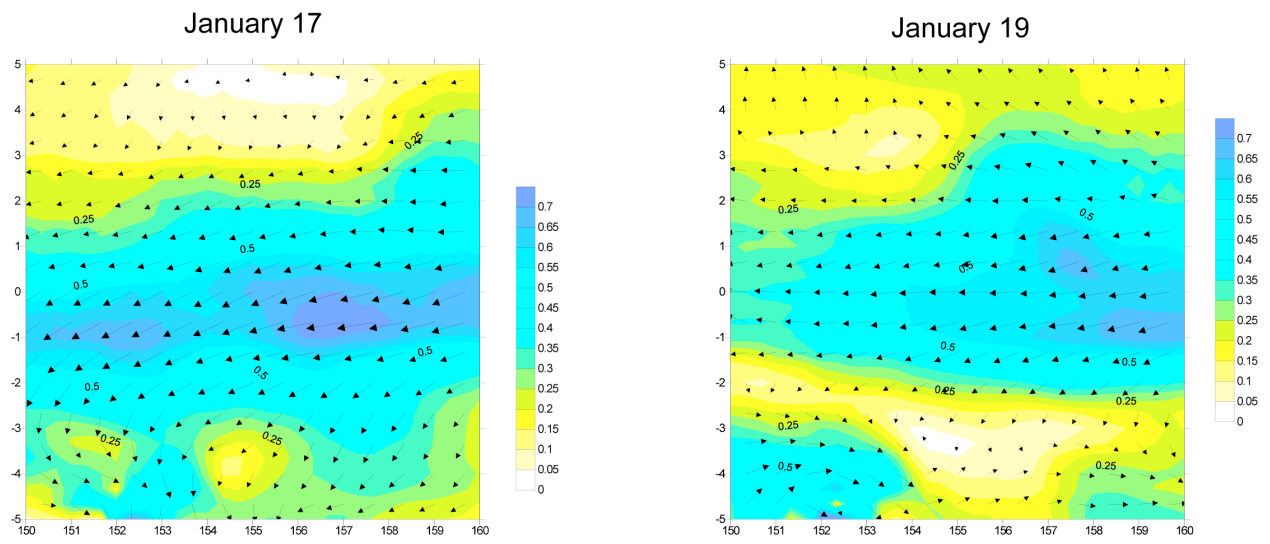


Figure 3. Daily-averaged surface currents from 17 January and 19 January.

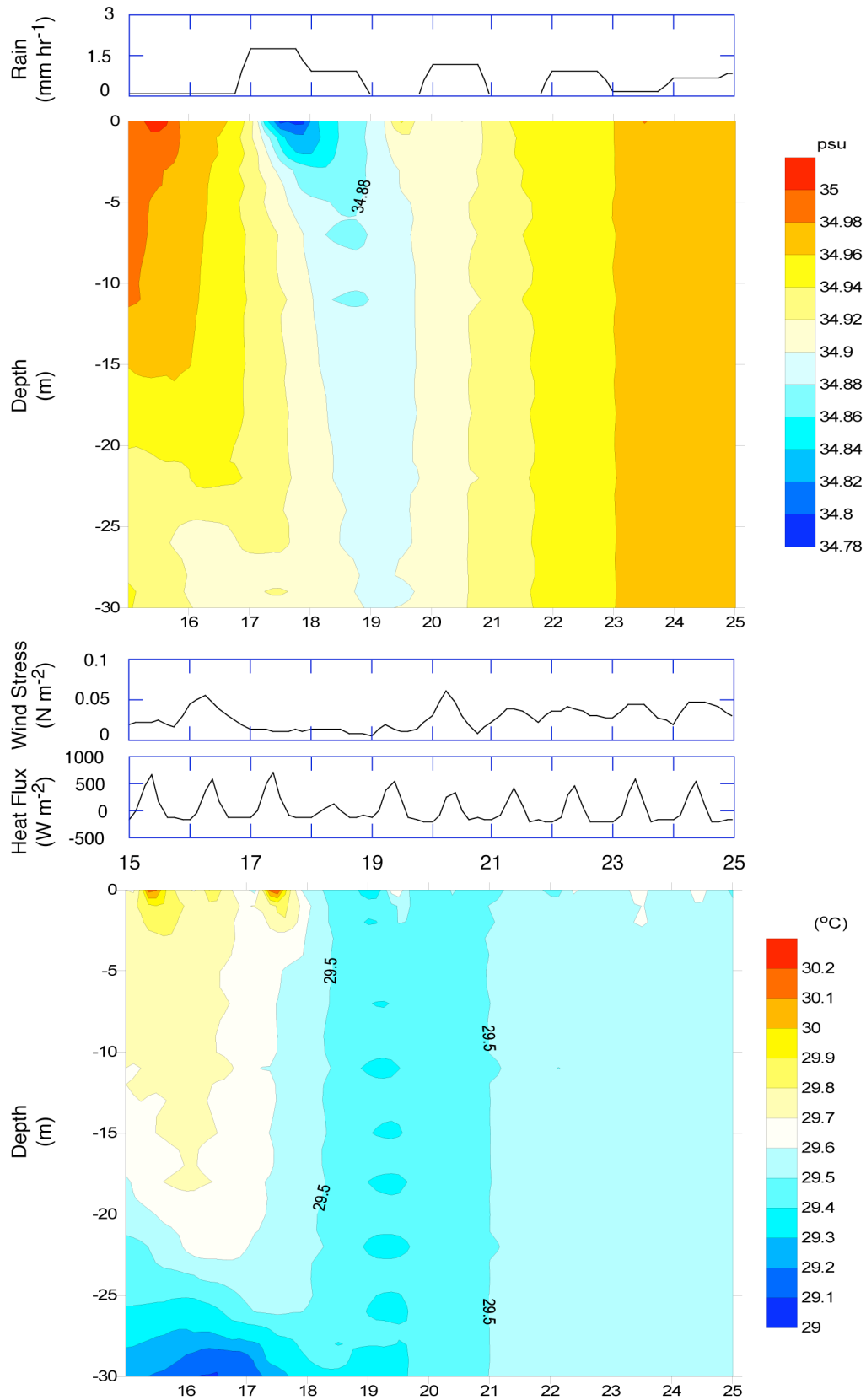


Figure 4. Time series of (from top) precipitation, salinity with depth, wind stress, surface heat flux (positive into the ocean), and temperature with depth.